Automated planning approaches for non-invasive cardiac valve replacement procedures from CT angiography

Gao, X.; Gao X.

5

Quantification of Aortic Annulus in Computed Tomography Angiography: Validation of a Fully Automatic Methodology

Xinpei Gao, Sara Boccalini, Pieter H. Kitslaar, Ricardo P.J. Budde, Mohamed Attrach, Shengxian Tu, Michiel A. de Graaf, Tomas Ondrus, Martin Penicka, Arthur J.H.A. Scholte, Boudewijn P.F. Lelieveldt, Jouke Dijkstra, Johan H.C. Reiber

Abstract

Background: Automatic accurate measuring of the aortic annulus and precise determination of the optimal angulation of X-ray projection are important for the trans-catheter aortic valve replacement (TAVR) procedure. The objective of this paper was to present a novel fully automatic methodology for the quantification of the aortic annulus in computed tomography angiography (CTA) images.

Methods: CTA datasets of 26 patients were analyzed retrospectively with the proposed methodology, which consists of a knowledge-based segmentation of the aortic root and detection of the orientation and size of the aortic annulus. The accuracy of the methodology was determined by comparing the automatically derived results with the reference standard obtained by semi-automatic delineation of the aortic root border and manual definition of the annulus plane.

Results: The difference between the automatic annulus diameter and the reference standard by observer 1 was 0.2 ± 1.0 mm, with an inter-observer variability of 1.2 ± 0.6 mm. The Pearson correlation coefficient for the diameter was good (0.92 for observer 1). For the first time, a fully automatic tool to assess the optimal projection curves was presented and validated. The mean difference between the optimal projection curves calculated based on the automatically defined annulus plane and the reference standard was 6.4º in the cranial/caudal (CRA/CAU) direction. The mean computation time was short with around 60 seconds per dataset.

Conclusion: The new fully automatic and fast methodology described in this manuscript not only provided reliable measurements about the aortic annulus size with results comparable to experienced observers, but also predicted optimal X-ray projection curves from CTA images.

European Journal of Radiology, August 2017, Volume 93, Pages 1–8, 2017. DOI: http://dx.doi.org/10.1016/j.ejrad.2017.04.020

5.1 Introduction

During TAVR procedure, the aortic root is not directly visible for physicians, thus pre-operative imaging is principal to determine the size and orientation of the aortic annulus. These measurements are essential to select and deliver the appropriate prosthesis in the aortic valve. Bias in the selection and placement of the prosthesis, may result in complications e.g. aortic annulus rupture, prosthesis shift or paravalvular regurgitation.

As a noninvasive, high-resolution 3D imaging modality, computed tomography (CT) enables the accurate imaging of the anatomical structures of the aortic root (Achenbach et al. 2012). The orientation of the aortic root can be determined manually from the CTA dataset in order to predict the optimal X-ray projection angle during prosthesis implantation in the Cath lab. An optimal X-ray projection curve with multiple available angles can be useful for physicians to choose their familiar angles (Gurvitch et al. 2010).

This reduces procedure time, the volume of contrast material used and radiation dose. However, in order to avoid the potential reproducibility issues of a manual measurement and to achieve faster reporting time, a fully automatic aortic root analysis methodology based on CTA images would be promising.

In this paper, we put forward a novel fully automatic methodology which is able to size the aortic annulus, and predict the optimal projection curve based on CTA image. The results were validated in datasets from two clinical centers to investigate its accuracy and robustness.

5.2 Materials and methods

Study population and CT protocol

26 patients from two hospitals were candidates for TAVR and underwent an ECG-gated CTA scan as the routine clinical investigation. The patients' identifiable information was completely anonymized before this study started. Table 5.1 describes the scan protocols for the CTA scans used in this study. Diastolic phases from the reconstructed images were used.

	Hospital A	Hospital B
Number of patients	19	7
CT scanner	320-row detector	128 x2 detector
	Single source	Dual source
	Aquilion ONE	Somatom Definition Flash

	Toshiba Medical System, Otowara, Japan	Siemens Healthcare, Forchheim, Germany
Acquisition	R-R full dose, in most cases no ECG modulation.	Prospective ECG-gating
Scan parameter‡	100, 120kV or 135kV, 400-580mA	100,120kV, 350–400mA
Injection protocol	bi-phasic injection	bi-phasic injection
	Intravenous in ante-cubital vein	Intravenous in ante-cubital vein
	70ml contrast (5ml/sec) and 50ml saline (5ml/sec)	90ml contrast(4ml/sec) and 100ml saline (4ml/sec)
Reconstruction parameter	slice thickness 0.5mm, interval 0.25mm	slice thickness 0.75mm, with 0.4mm increment

‡ Tube voltage and current were adapted for each patient on the basis of body mass index (BMI) and thoracic anatomy.

Table 5.1 CTA protocols of the two clinical centers

Fully automatic aortic annulus detection framework

In a previously published study (Gao, Kitslaar, Scholte, et al. 2016), we described a fully automatic segmentation method for pre-TAVR whole-body CTA datasets with a high mean dice similarity coefficient (0.965 ± 0.024) of the contours of the automatic methodology and the reference. In this study, an adapted framework based on the previous method was used for segmentation of the aortic root in the cardiac CTA images.

The procedure for automatic annulus detection works as follows: first, the data sets were resampled and the heart region was masked out automatically by a deformable subdivision surface fitting algorithm (Gao, Kitslaar, Scholte, et al. 2016). Then, the three-dimensional contours of the aortic root, as well as left ventricle outflow tract (LVOT) were detected with an atlas-based segmentation algorithm. Eight cardiac CTA images with manual annotations were used as the atlas images. Each patient's image was registered to the atlas images by an affine registration algorithm. The most similar atlas image was selected based on the similarity measure (Mutual information) of the atlas image and the patient image for a subsequent B-Spline deformation registration algorithm (Klein et al. 2010). After registration, the manual segmentation of the selected atlas image was

deformed by the transformation parameters from previous steps, therewith the patient's image was initially segmented. Finally, we refined the segmentation by an adaptive subdivision surface model fitting method based on gradient information (Kitslaar et al. 2015).

The automatic extraction of the aortic annulus depend on the anatomy of the aortic root. The aortic root is a complex 3-dimensional structure that starts at the left ventricle outflow tract (LVOT). It consists of the sinotubular junction, aortic sinuses of Valsalva, as well as valve leaflets (Underwood et al. 2000). The aortic annulus plane is a suppositional plane composed by the hinge points of the leaflets beyond the LVOT. It can also be called 'basal ring' (Schoenhagen, Hausleiter, et al. 2011). The prosthesis is settled on the location of the aortic annulus during the TAVR procedure.

After the extraction of the aortic root and the LVOT by the atlas-based segmentation, we calculated the connecting region between the aortic root and the LVOT. By applying the principal component analysis (Shlens 2014), the orientation of the connecting region between the aortic root and the LVOT can be found, which defines the orientation of the annulus plane.

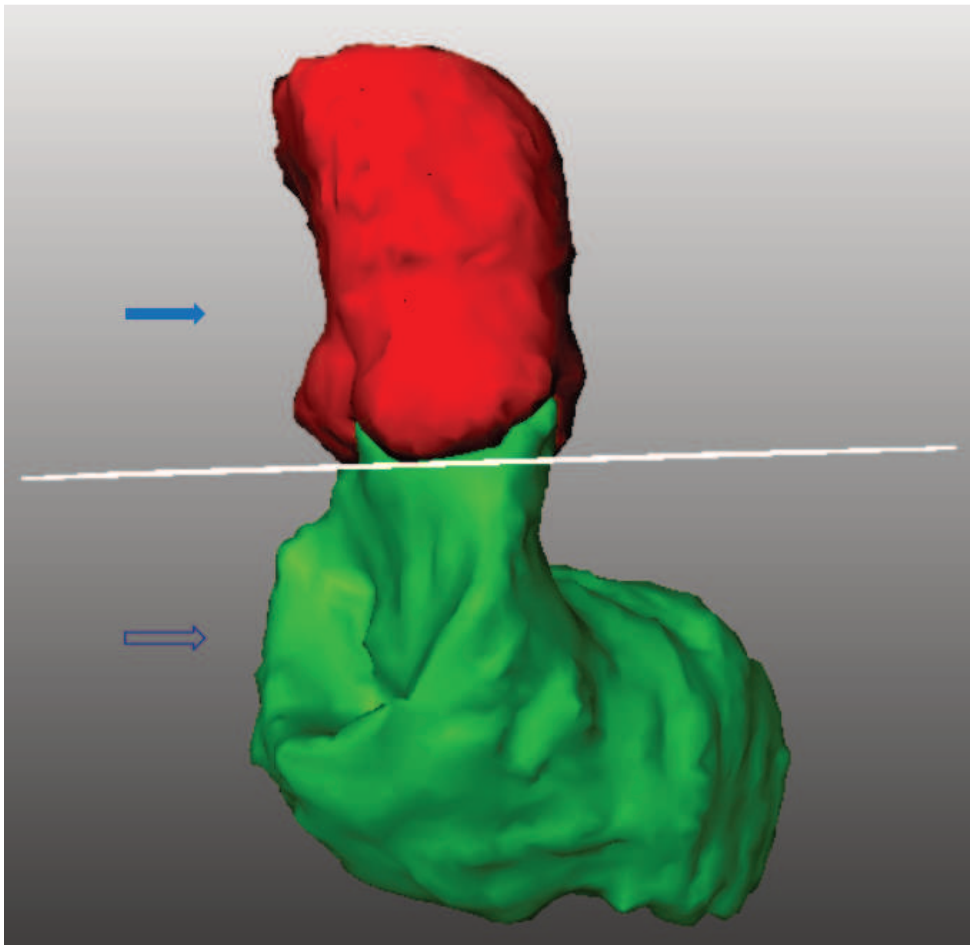

Figure 5.1 - Annular plane detection: the red top part represents the segmentations of the aortic root (solid arrow) and green low part LVOT (hollow arrow), the white plane corresponds to the plane of the aortic annulus.

Prediction of optimal projection curve for X-ray

The identification of X-ray projections orthogonal to the aortic annular plane is important for the correct valve deployment during the TAVR procedure. With the orientation of the aortic annulus plane computed in the previous step, an infinite number of projections can be calculated which allows the 3 hinge points of the valves to appear on the same line in the X-ray projection view (Kurra et al. 2010). An optimal projection curve with left/right anterior oblique (LAO/RAO) angles as the x-axis, and cranial/caudal (CRA/CAU) angles as the y-axis, was calculated. Following the diagram style employed in the study by Binder et al (Binder et al. 2012), LAO/RAO angles ranging from 45° RAO to 45° LAO were represented with 5° steps. Based on these LAO/RAO angles, each patient's CRA/CAU angles were computed (Figure 5.2).

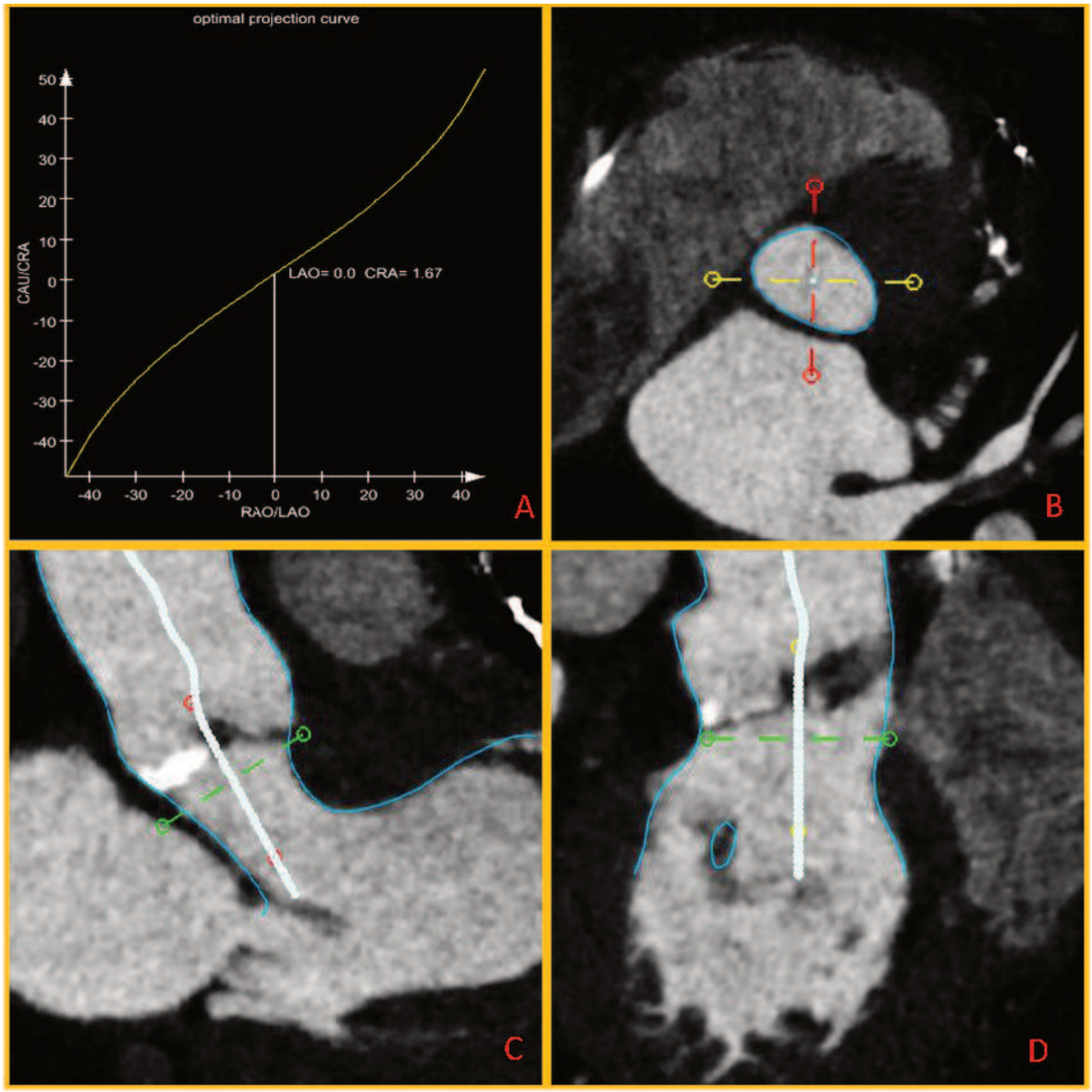

Figure 5.2 - The optimal projection curve and related images: A - the optimal projection curve; B – multi-planar image of the annulus plane; C – oblique image

corresponding to the optimal X-ray projection D – oblique image perpendicular to image B & C.

Evaluation of aortic annulus detection

The automatic methodology was integrated into a dedicated in-house tool (AortaValveViewer 1.2, LKEB, Leiden, Netherlands), with functions for manual interactions. The tool was implemented in the MeVisLab environment (version 2.7.1, MeVis Medical Solutions AG, Bremen, Germany) with C++ and Python code.

Two observers performed the measurements for the evaluation of the performance of our automatic methodology (both of them have at least 4 years' experience working in cardiovascular imaging and 100 annulus diameters assessments). The two observers used the in-house tool independently to create reference standards for statistical analysis. The observer adjusted double oblique multiplanar reconstruction (MPR) images manually to find the plane in which the three aortic valve hinge points appear in the same slice. Three landmarks were annotated manually on the hinge points, which defined the annulus plane. Then the observer corrected the automatically segmented surface from the sinotubular junction to the LVOT (5mm under the aortic annulus) by drawing contours in cross-sectional and oblique view images (Figure 5.2 B, C & D).

The annular cross-sectional contour was extracted from the aortic root segmentation where it intersected with the annulus plane. The size of the aortic annulus was surveyed using the area, radius, diameter, long-axis diameter (LAD), as well as short-axis diameter (SAD) and perimeter. The radius (R) of the aortic annulus was calculated based on the area (A): $R = \sqrt{(A/\pi)}$; the diameter was obtained based on the radius (D): $D = 2R$.

The center of the annulus was defined as the center of its contour and automatically calculated. Next, the angle between automatic and manual plane orientations, the 3D Euclidean distance between the centers of the annulus contours obtained from the automatic and manual planes were measured (Deza and Deza 2009). In addition, the optimal X-ray projection curve was calculated for each patient from the automatic and manual plane orientations by observer 1. The mean optimal X-ray projection curve of all the patients was obtained. Automatic and manual curves were compared with each other in the CRA/CAU axis.

A four points scale quality score (4 = perfect, 3 = good, 2 = reasonable, 1 = poor) based on motion artifacts and contrast in the aortic root was used to evaluate the image quality by observer 1. The extent of the calcification in the aortic root at the level of the annulus or immediately nearby (caudal part of the cusps and cranial LVOT) was graded into 4 levels: 1 = none, 2 = light, 3 = medium, 4 = heavy.

Evaluation of prosthesis size selection

The sizes of the prosthesis which had been implanted during the TAVR procedure into the patients from hospital A were retrieved. The selection of the prosthesis performed in clinical practice was retrospectively compared with a theoretical choice of the valve based on the automatic and semi-automatic annulus measurements of our tool. The annulus area measurements of the in-house tool were categorized based on the commercially available valve sizes: 23, 26, 29 mm for the Edwards SAPIEN XT valves and 23, 26, 29, 31 mm for the CoreValve (Kasel et al. 2013; Lou et al. 2015). Prosthesis selection based on area measurements is summarized in Table 5.5 and 5.6. If the measurement fell into the gray zone, both prostheses with smaller or bigger size were considered as suitable.

Edwards SAPIEN Valve (mm)	23	gray zone	26	gray zone	29
Area (mm^2)	300 - 380	380 - 415	415 - 490	490 - 530	530 - 620

Table 5.5 Selection table for Edwards SAPIEN XT valve

Core Valve (mm)	23	26	29	31
Area (mm2)	254.5 - 314.2	314.2 – 415.5	415.5 – 572.6	530.9 – 660.5

Table 5.6 Selection table for Core valve

Statistical analysis

In this study, SPSS (version 20.0, SPSS Inc., Chicago, IL) were used for the statistical analyses, along with MedCalc (version 15.6, Ostend, Belgium). The variables were analyzed by the mean, standard deviation (SD), and the Pearson correlation coefficient if normally distributed and continuous. The normality was evaluated by the Shapiro-Wilk test (Shapiro and Wilk 1965). Bland-Altman plots were drawn to visualize the bias. P value < 0.05 indicated significant result.

5.3 Results

This study population consists of 26 patients, and the baseline characteristics are described in Table 5.2. The patients differ in age, gender, as well as the existence of previous percutaneous coronary intervention (PCI), previous myocardial infarction (MI) and previous coronary artery bypass grafting (CABG), in other words, a population with pathological diversity.

Patient number	Total (26)
Age (years)	79 ± 13
Gender (% male)	15 (58%)
Diabetes	4 (15%)
Hypertension	17 (65%)
Hypercholesterolemia	16 (62%)
Family history of CAD	3 (12%)
Smoking	2 (8%)
Obesity	5 (19%)
Previous PCI	13 (50%)
Previous CABG	12 (46%)
Previous MI	5 (19%)

In the data, age is described by mean ± SD, other items are outlined by percentages of the population.

Table 5.2 Baseline Characteristics of the patients in the study

Image quality score and calcification level

The average image quality score was 2.4. The percentage of scans with poor image quality was 15%, reasonable 42%, good 31%, and perfect 12%. The average score of images from hospital A was 2.6, the mean score of hospital B was 1.9. Only 1 patient had no calcification (4%). The amount of calcification in the remaining patients was light in 12 cases (46%), medium in 10 cases (39%) and heavy in 3 patients (12%). The mean calcification amount of all the patients was light to medium (2.6) with a lower average value for patients scanned at hospital A (2.4) compared to hospital B (3.1).

Accuracy of the orientation of the aortic annulus

The difference between the annulus plane orientations was 9.4 ± 4.6 degrees for observer 1, and 7.6 ± 3.7 degrees for observer 2, with 4.2 ± 3.3 degrees for the inter-observer variability. The average and standard deviation of the distance between the automatic and manual annulus center locations was found to be 1.7 ± 1.0 mm for observer 1, 1.6 ± 1.0 mm for observer 2, and the inter-observer variability was 1.2 ± 0.7 mm. The individual errors are presented in Figure 3, where the patients are represented by numbers. For patients 13 and 19 with an associated error higher than 15 mm, the image quality was poor. For patients 10 and 26, who presented an error for the location of the center higher than 3mm, the image quality was reasonable.

For the patients from hospital A, the average error of the plane orientation was 9.0 degrees for observer 1 and 7.2 degrees for observer 2; for patients from hospital B, the mean error of the orientation was 10.4 degrees for observer 1 and 8.2 degrees for observer 2.

Assessment of the optimal projection curve

In Figure 5.4, the mean optimal projection curves of the patients from the automatic methodology and observer 1 are presented together with their standard deviations. The mean difference in CAU/CRA for all the patients was 6.4 degree. The standard deviations of the two curves were similar to each other, representing the range of the CAU/CRA angle in all the patients.

Evaluation of the size of the aortic annulus

Area, radius, diameter, LAD, SAD, and perimeter were calculated for the evaluation of the aortic annulus size measurement. Table 5.3 shows the mean, standard deviation and 95% CI of these parameters of the automatic measurement and the two observers. Table 5.4 shows the Pearson correlation coefficient and difference (mean ± SD) of the parameters between the automatic measurement and the reference standards. Figure 5.5 shows the Bland-Altman plots for all the annulus size measurements (automatic VS observer 1).

Evaluation of prosthesis size selection

Based on our fully-automatic measurement, in 78.9% (15 out of 19) of cases the selection of the prosthesis size would have been the same as in clinical practice. When observer 1 applied corrections to the fully-automatic measurement, the agreement rate increased to 89.5% (17 out of 19).

Computation time of the method

Our automatic methodology takes around 60 seconds to detect the contour of the aortic root and measure the aortic annulus in one dataset on

a workstation. Observers needed on average 12 minutes to generate the reference standard.

5.4 Discussion

In recent years, many studies have been published on aortic annulus size quantification based on CTA images, for the evaluation and validation of both semi-automatic (Delgado et al. 2011; Foldyna et al. 2015; Stortecky et al. 2014; Watanabe et al. 2013) and fully-automatic (Mustafa Elattar et al. 2016; El Faquir et al. 2016; Ionasec et al. 2010; Lou et al. 2015; Wächter et al. 2010) tools. Fully automatic tools require less user interaction for the physicians. In our study, the main goal was to evaluate our tool for fully automatic annulus size quantification. Ionasec et al. (Ionasec et al. 2010) developed a system to model and quantify the left heart valves. In their study the precision of the annular circumference was 8.46 ± 3.0 mm. Elattar et al. (Mustafa Elattar et al. 2016) introduced an automated detection method which enabled automated sizing based on Normalized cut, and Gaussian curvature map. The automatically generated aortic annulus radius' average difference was 0.2 ± 0.7 mm with observer 1, and 0.4 ± 0.8 mm with observer 2. Lou et al. (Lou et al. 2015) evaluated the results of fully automatic aortic annulus sizing from a commercial tool, and reported an area measurement calculated by observer 1 with the automated method without manual correction of 5.4 ± 0.96 cm2, and of 4.8 ± 0.87 cm2 with manual correction; with the same methods, observer 2 obtained area values of 5.4 ± 0.95 cm2 versus 5.0 ± 0.91 cm2. Wachter et al. (Wächter et al. 2010) used a model-based algorithm to detect the aortic valve anatomy, obtaining errors for the short and long diameters of the annulus of 0.8 and 1.0 mm, respectively. In Queirós et al.'s study (Queirós et al. 2016), the area-derived diameter calculated by the automatic aortic root algorithm was compared with manual results from two observers, the difference was 0.08 mm for the observer 1 and 0.25 mm for the observer 2. Our framework can detect the aortic root in all the patients, the correlation of the diameter was good, and the errors of the aortic annulus size parameters were small, comparable with previous studies (Mustafa Elattar et al. 2016; Ionasec et al. 2010; Lou et al. 2015; Wächter et al. 2010) and comparable to the human observer difference (Table 4).

Just a few studies about optimal X-ray projection curve prediction were published (El Faquir et al. 2016; Samim et al. 2013). In Faquir et al.'s study (El Faquir et al. 2016), the optimal projection curves of the automated software were calculated based on the aortogram, not on CTA images. The median difference between the optimal projection curves of the automated software calculated based on the aortogram and manual ground-truth was

8.8 and 14.6 degrees in two different cohorts. In Samim et al.'s study (Samim et al. 2013), the calculation was based on CTA images, however, the prediction of optimal projection curves was not performed fully automatically. The novelty of the present study consists in the fact that for the first time a fully automatic tool is presented which can perform the optimal projection curve prediction on CTA images.

In the study by Lou et al. (Lou et al. 2015), the influence of the measurement on the prosthesis size selection was also evaluated. For the first observer, the fully automated and the manual measurements agreed on the prosthesis selection in 51.8% of the patients, while the agreement of the semi-automated and the manual measurements was 87.6%. For the second observer, the fully-automated and the manual measurement agreed in 52.8% of the cases, while the agreement of the semi-automated and the manual measurement was 82.4%. In our study, the agreement rate between our fully automatic measurement and clinical practice was 78.9%, and between our semi-automatic measurement and clinical practice 89.5%.

Due to the broader employment of the TAVR procedure and the subsequent increase in the number of pre-procedural CT scans, the images processing time is becoming crucial. According to Elattar et al.'s description (M a Elattar et al. 2014), their automatic contour detection of the aortic root took 90 seconds without the detection of the aortic annulus and the calculation of the clinical parameters in the aortic root. In our study, the average computation time including aortic root segmentation, automatic detection, and calculation of the clinical parameters of the aortic annulus was shorter (around 60 seconds) and can be further improved.

Only diastolic images were used in this study. There have been studies which investigated the impact of using diastolic and systolic images on prosthesis sizing (Bertaso et al. 2012; Blanke et al. 2012; De Heer et al. 2011). Bertaso et al. (Bertaso et al. 2012) measured the difference of aortic annulus size between diastole and systole, and found that the difference was not significant enough to change prosthesis size selection; while in de Heer et al.'s study (De Heer et al. 2011), the opposite conclusion was reached. In Blanke et al.'s study (Blanke et al. 2012), the annulus was measured throughout the full cardiac cycle, and it turned out that the phase in which the annulus has the biggest size would be the most suitable phase for prosthesis selection. However, this ideal phase can be diastolic or systolic depending on the patient. The method presented in this study can be used for automatic annulus measurement in patients whose ideal phase is in diastole.

In our study, two kinds of CT scanners (Aquilion ONE scanner and Somatom Definition Flash scanner) with different acquisition protocols were

used from two hospitals. The patients who were scanned in hospital A had a higher image quality and a lower amount of calcium. Image quality had an impact on our automatic tool. The angulation results were better in the patients from hospital A, where an Aquilion ONE scanner was used. However, the 3 patients with the heavy calcifications did not show higher error, which indicates that our framework is not influenced by calcification.

The current study has a number of limitations. Firstly, given the limited number of data sets, the robustness of the method cannot be adequately assessed. We plan to investigate this in a more extensive study with more data. Secondly, the automatic measurement of the sinotubular junction, sinus of Valsalva and LVOT have been developed in our methodology, but not validated in this study. Finally, the optimal projection curve has not been compared with the actual projection during the TAVR procedure in the Cath lab.

5.5 Conclusion

Our newly developed methodology of automatic aortic annulus quantification on CTA images has been demonstrated to be accurate compared to the semi-automatic results. A fully automatic optimal X-ray projection curve prediction algorithm based on CT image was described. Our methodology provides physicians with information about the size and orientation of the aortic annulus in detail, which can help with the prosthesis selection in the pre-operative planning of TAVR.

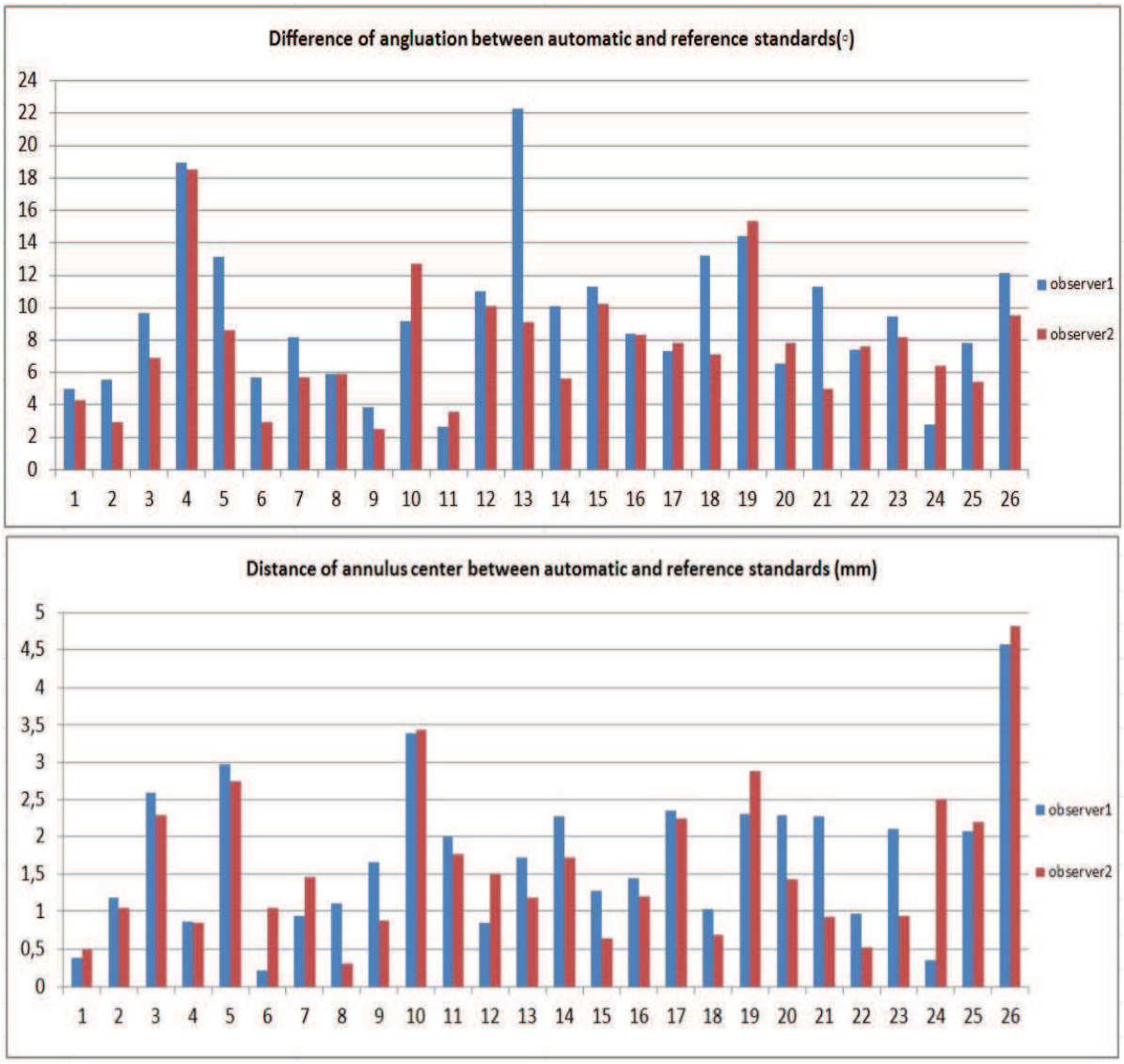

Figure 5.3 - The difference in the degree of the aortic annulus orientation between automatic and the observers.

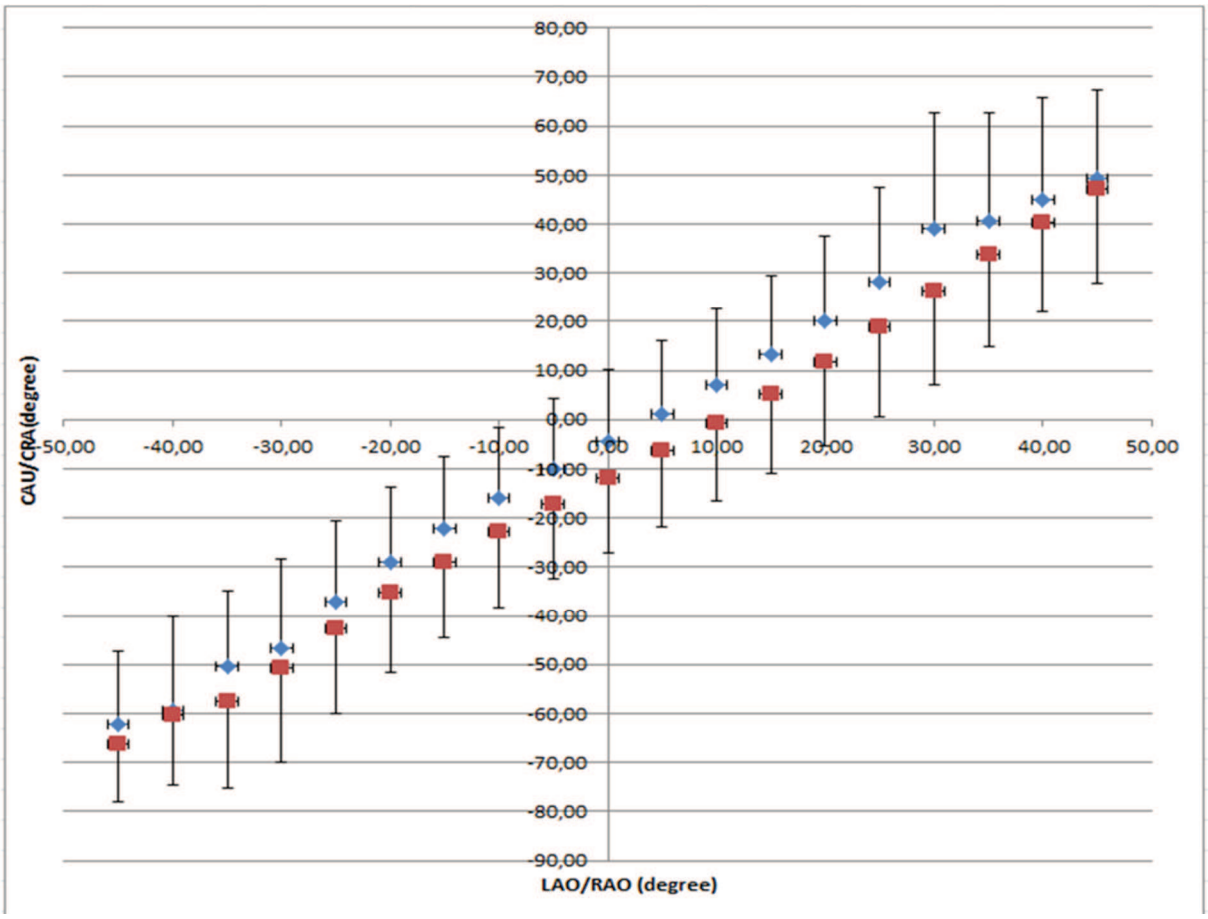

Figure 5.4 - Optimal projection curve: the mean optimal projection curve of the CAU/CRA angulation of automatic measurement (blue) and observer's measurement (red). The horizontal bars above the blue dots show the SDs of automatically extracted CAU/CRA of all the patients. The bars beneath the red dots represent the SDs of the observer's measurement.

Aortic annulus		Automatic measurement			Observer 1			Observer 2		
	unit	mean	SD	95% CI	mean	SD	95% CI	mean	SD	95% CI
Area	cm^2	4.8	1.0	4.4 to 5.2	4.7	1.0	4.3 to 5.1	5.1	1.0	4.7 to 5.6
Radius	mm	12.3	1.3	11.7 to 12.8	12.1	1.3	11.6 to 12.7	12.8	1.3	12.2 to 13.2
Diameter	mm	24.5	2.6	23.5 to 25.6	24.3	2.6	23.2 to 25.3	25.5	2.6	24.4 to 26.5
Long-axis diameter	mm	30.5	4.4	28.8 to 32.3	29.9	3.5	28.5 to 31.3	31.1	3.3	29.8 to 32.5
Short-axis diameter	mm	21.4	2.6	20.4 to 22.4	21.1	2.5	20.1 to 22.1	22.2	2.5	21.2 to 23.1
perimeter	mm	80.3	9.5	76.4 to 84.1	78.5	8.2	75.2 to 81.8	82.1	8.0	78.9 to 85.3

Table 5.3 Results of the detection of aortic annulus size from automatic measurement and reference standard.

Aortic annulus		Automatic VS Observer 1		Automatic VS Observer 2		Observer 1 VS Observer 2	
	unit	Correlation	Difference (mean ± SD)	Correlation	Difference (mean ± SD)	Correlation	Difference (mean ± SD)
Area	cm^2	0.92	0.1 ± 0.4	0.89	0.4 ± 0.5	0.97	0.5 ± 0.2
Radius	mm	0.91	0.1 ± 0.5	0.88	0.5 ± 0.6	0.97	0.6 ± 0.3
Diameter	mm	0.91	0.2 ± 1.0	0.88	1.0 ± 1.2	0.97	1.2 ± 0.6
Long-axis diameter	mm	0.85	0.7 ± 2.3	0.78	0.6 ± 2.8	0.94	1.2 ± 1.2
Short-axis diameter	mm	0.82	0.3 ± 1.5	0.78	0.8 ± 1.7	0.96	1.0 ± 0.7
Perimeter	mm	0.82	1.8 ± 5.5	0.81	1.8 ± 5.5	0.97	3.6 ± 2.0

Table 5.4 Results of aortic annulus size measurement comparing the automatic measurement to reference standard.

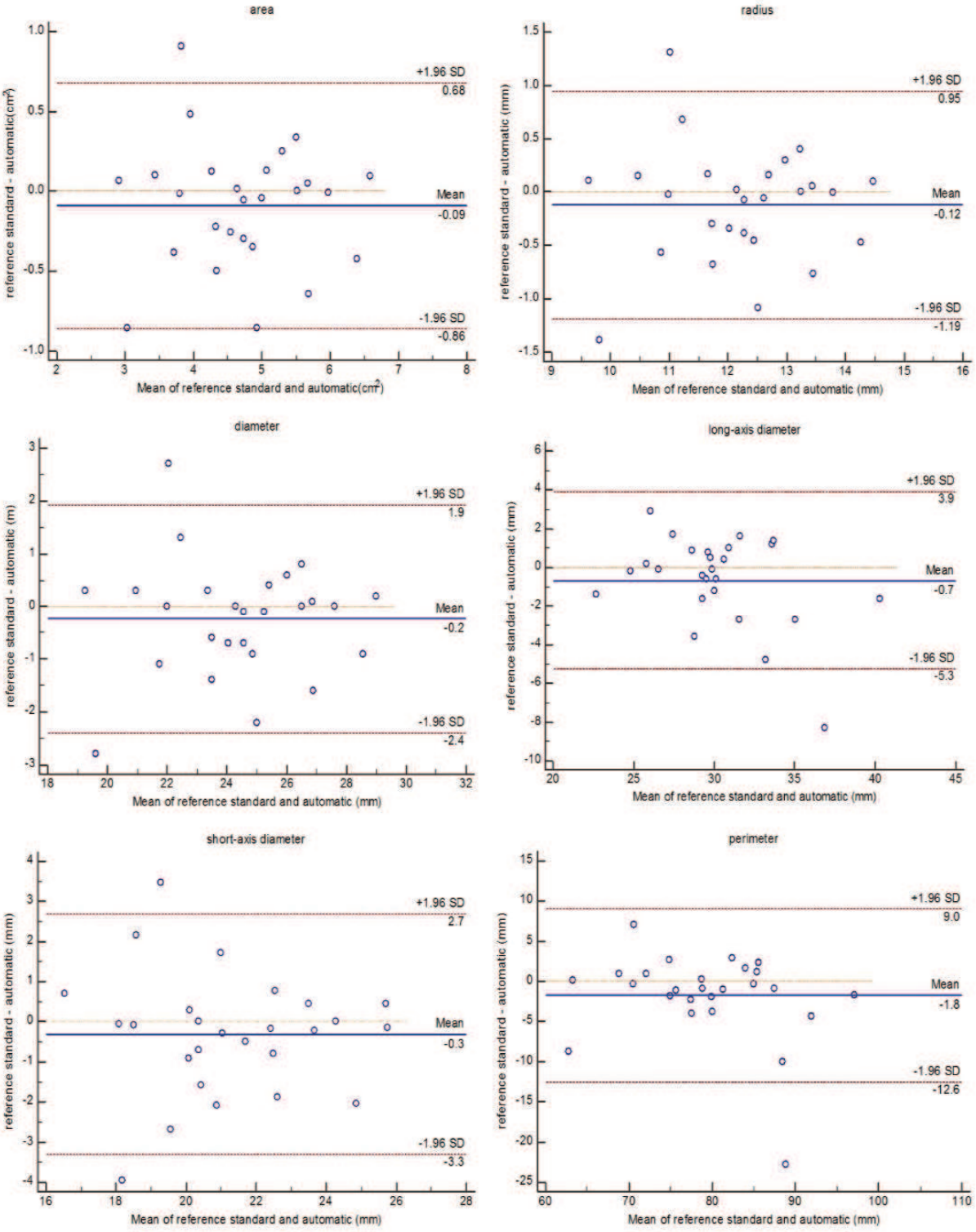

Figure 5.5 Bland-Altman plots of aortic annulus parameters